Characterized Brillouin scattering in silica optical fiber tapers based on Brillouin optical correlation domain analysis

Weiwen Zou,* Wenning Jiang, and Jianping Chen

State Key Laboratory of Advanced Optical Communication Systems and Networks, Department of Electronic Engineering, Shanghai Jiao Tong University, Shanghai 200240, China
wzou@sjtu.edu.cn

Abstract: This paper demonstrates stimulated Brillouin scattering (SBS) characterization in silica optical fiber tapers drawn from commercial single mode optical fibers by hydrogen flame. They have different waist diameters downscaled from 5 μm to 42 μm. The fully-distributed SBS measurement along the fiber tapers is implemented by Brillouin optical correlation domain analysis technique with millimeter spatial resolution. It is found that the Brillouin frequency shift (BFS) in the waist of all fiber tapers is approximately the same (i.e., ~11.17 GHz at 1550 nm). However, the BFS is gradually reduced and the Brillouin gain decreases from the waist to the untapered zone in each fiber taper.

OCIS codes: (290.5900) Scattering, stimulated Brillouin; (120.5820) Scattering measurements; (060.2400) Fiber properties; (060.4370) Nonlinear optics, fibers.

References and links

1. L. M. Tong, R. R. Gattass, J. B. Ashcom, S. He, J. Lou, M. Shen, I. Maxwell, and E. Mazur, "Subwavelength-diameter silica wires for low-loss optical wave guiding," Nature **426**(6968), 816–819 (2003).
2. W. J. Wadsworth, A. Ortigosa-Blanch, J. C. Knight, T. A. Birks, T. P. M. Man, and P. S. J. Russell, "Supercontinuum generation in photonic crystal fibers and optical fiber tapers: a novel light source," J. Opt. Soc. Am. B **19**(9), 2148–2155 (2002).
3. G. Humbert, W. Wadsworth, S. Leon-Saval, J. C. Knight, T. A. Birks, P. St J Russell, M. Lederer, D. Kopf, K. Wiesauer, E. Breuer, and D. Stifter, "Supercontinuum generation system for optical coherence tomography based on tapered photonic crystal fibre," Opt. Express **14**(4), 1596–1603 (2006).
4. W. Long, W. Zou, X. Li, and J. Chen, "DNA optical nanofibers: preparation and characterization," Opt. Express **20**(16), 18188–18193 (2012).
5. Y. W. Song, K. Morimune, S. Y. Set, and S. Yamashita, "Polarization insensitive all-fiber mode-lockers functioned by carbon nanotubes deposited onto tapered fibers," Appl. Phys. Lett. **90**(2), 021101 (2007).
6. J. Villatoro, V. Finazzi, V. P. Minkovich, V. Pruneri, and G. Badenes, "Temperature-insensitive photonic crystal fiber interferometer for absolute strain sensing," Appl. Phys. Lett. **91**(9), 091109 (2007).
7. H. Luo, X. Li, W. Zou, X. Li, Z. Hong, and J. Chen, "Temperature-insensitive micro-displacement sensor based on locally bent microfiber taper modal interferometer," IEEE Photon. J. **4**(3), 772–778 (2012).
8. P. Polynkin, A. Polynkin, N. Peyghambarian, and M. Mansuripur, "Evanescent field-based optical fiber sensing device for measuring the refractive index of liquids in microfluidic channels," Opt. Lett. **30**(11), 1273–1275 (2005).
9. C. Grillet, C. L. C. Smith, D. Freeman, S. Madden, B. Luther-Davies, E. Magi, D. Moss, and B. Eggleton, "Efficient coupling to chalcogenide glass photonic crystal waveguides via silica optical fiber nanowires," Opt. Express **14**(3), 1070–1078 (2006).
10. G. P. Agrawal, *Nonlinear Fiber Optics*, 4th ed. (Academic Press, 2007).
11. A. Kobyakov, S. Kumar, D. Q. Chowdhury, A. B. Ruffin, M. Sauer, S. R. Bickham, and R. Mishra, "Design concept for optical fibers with enhanced SBS threshold," Opt. Express **13**(14), 5338–5346 (2005).
12. W. Zou, Z. He, and K. Hotate, "Investigation of strain- and temperature-dependences of Brillouin frequency shifts in GeO_2-doped optical fibers," J. Lightwave Technol. **26**(13), 1854–1861 (2008).
13. Y. Mizuno, P. Lenke, K. Krebber, and K. Nakamura, "Characterization of Brillouin gain spectra in polymer optical fibers fabricated by different manufacturers at 1.32 and 1.55 μm," IEEE Photon. Technol. Lett. **24**(17), 1496–1498 (2012).
14. D. Garcus, T. Gogolla, K. Krebber, and F. Schliep, "Brillouin optical-fiber frequency-domain analysis for distributed temperature and strain measurements," J. Lightwave Technol. **15**(4), 654–662 (1997).

#183374 - $15.00 USD Received 14 Jan 2013; revised 8 Feb 2013; accepted 28 Feb 2013; published 7 Mar 2013

15. X. Bao, A. Brown, M. Demerchant, and J. Smith, "Characterization of the Brillouin-loss spectrum of single-mode fibers by use of very short (<10-ns) pulses," Opt. Lett. **24**(8), 510–512 (1999).
16. K. Hotate and T. Hasegawa, "Measurement of Brillouin gain spectrum distribution along an optical fiber using a correlation-based technique - proposal, experiment and simulation," IEICE Trans. Electron. **E83-C**, 405–412 (2000).
17. W. Zou, Z. He, and K. Hotate, "Complete discrimination of strain and temperature using Brillouin frequency shift and birefringence in a polarization-maintaining fiber," Opt. Express **17**(3), 1248–1255 (2009).
18. W. Zou, Z. He, and K. Hotate, "Demonstration of Brillouin distributed discrimination of strain and temperature using a polarization-maintaining optical fiber," IEEE Photon. Technol. Lett. **22**(8), 526–528 (2010).
19. Y. Mizuno, W. Zou, Z. He, and K. Hotate, "Proposal of Brillouin optical correlation-domain reflectometry (BOCDR)," Opt. Express **16**(16), 12148–12153 (2008).
20. W. Zou, C. Jin, and J. Chen, "Distributed strain sensing based on combination of Brillouin gain and loss effects in Brillouin optical correlation domain analysis," Appl. Phys. Express **5**(8), 082503 (2012).
21. J. Chen, X. Shen, Z. Hong, and X. Li, "Nanostructure optic-fiber-based devices for optical signal processing," in *OptoeElectronics and Communications Conference (OECC 2010)*, pp. 550–551, invited paper 8E2–1.
22. W. Zou, Z. He, and K. Hotate, "Two-dimensional finite element modal analysis of Brillouin gain spectra in optical fibers," IEEE Photon. Technol. Lett. **18**(23), 2487–2489 (2006).
23. T. A. Birks and Y. W. Li, "The shape of fiber tapers," J. Lightwave Technol. **10**(4), 432–438 (1992).
24. J. E. McElhenny, R. K. Pattnaik, J. Toulouse, K. Saitoh, and M. Koshiba, "Unique characteristic features of stimulated Brillouin scattering in small-core photonic crystal fibers," J. Opt. Soc. Am. B **25**(4), 582–593 (2008).
25. T. Erdogan, "Cladding-mode resonances in short- and long-period fiber grating filters," J. Opt. Soc. Am. A **14**(8), 1760–1773 (1997).
26. http://www.mathworks.com/matlabcentral/fileexchange/27819-optical-fibre-toolbox
27. K. Y. Song, Z. Y. He, and K. Hotate, "Distributed strain measurement with millimeter-order spatial resolution based on Brillouin optical correlation domain analysis," Opt. Lett. **31**(17), 2526–2528 (2006).

1. Introduction

Optical fiber tapers can be downscaled to subwavelength diameter with low transmission loss [1]. Up to date, they can originate from whichever of all-silica fibers [1, 2], photonic crystal fibers [3], or even biomaterials (such as DNA) [4]. Due to the downscaled diameter, there is large evanescent optical field existing surrounding the taper's waist [1], which has excited a lot of research issues for developing the compact photonic components [2–9]. For instance, they are excellent candidates for supercontinuum generation [2, 3], passively mode-locked fiber laser [5], compact fiber-optic sensors [6–8], and nanowire connectors with photonic devices [9].

Stimulated Brillouin scattering (SBS) occurs in optical fibers when two counter-propagating optical waves have a precise frequency offset called Brillouin frequency shift (BFS), $\nu_B = 2n_{eff}V_a/\lambda$, where λ is the optical wavelength in vacuum, n_{eff} the effective refractive index of the fiber, and V_a the acoustic velocity [10, 11]. Both n_{eff} and V_a are determined by the fiber materials and optical/acoustic waveguide structure [10]. Recently, *Kobyakov et al.* proved that Brillouin gain is not just related to the optical effective area, but physically determined by the acouso-optic overlapping efficiency (or called the acousto-optic effective area) [11]. Consequently, the SBS measurement has been an effective tool to study the fiber properties [12, 13], and suitable to develop distributed strain and temperature sensing for structural health monitoring in smart materials and smart structure [14–20].

In this paper, we demonstrate the characterized SBS in silica optical fiber tapers based on Brillouin optical correlation domain analysis (BOCDA) technique. For the first time to our best knowledge, we experimentally investigate the SBS property in silica optical fiber tapers with different waist diameters from 5 μm to 42 μm, which are drawn from commercial single mode optical fibers (SMFs) by hydrogen flame [21]. The BFS in the tapers' waist is almost the same (i.e., ~11.17 GHz at 1550 nm), which is equal to the fourth-peak resonance frequency in the SMF [22]. The distributed measurement essentially explores the unique SBS properties of the fiber tapers rather than those of the untapered SMF.

2. Experimental setup

The experimental setup is depicted in Fig. 1. Distributed SBS measurement is based on the modified BOCDA technique [20]. A 1550-nm distributed-feedback laser diode (DFB-LD) is

#183374 - $15.00 USD Received 14 Jan 2013; revised 8 Feb 2013; accepted 28 Feb 2013; published 7 Mar 2013

used as the light source, which is divided into two coherent beams by a 3-dB coupler. It is noted that a function generator providing the sinusoidal frequency modulation is introduced or not introduced into the DFB-LD for distributed or entire SBS measurement [16], respectively. The upper and lower beams serve as SBS probe and pump waves, respectively. Before the probe beam enters unidirectionally into the fiber under test (FUT) through an isolator, a polarization scramble (PS) is used so as to average the possible polarization disorder in the FUT. Note that a ~5-km fiber spool is inserted in the upper beam for distributed SBS measurement to localize a higher-order correlation peak in the FUT [16, 20].

A dual-parallel Mach–Zehnder modulator (DMZM) is laid in the lower beam in order to generate a carrier-suppressed single sideband (CSSS) with upshifted frequency or a carrier-suppressed double sidebands (CSDS), which is determined by the bias voltage [20]. The upshifted frequency (i.e., the pump-probe relative frequency offset) is determined by the microwave synthesizer driving DMZM. A booster erbium-doped fiber amplifier (EDFA) is inserted after the DMZM to amplify the optical power.

The CSSS generation provides strong SBS amplification from the lower arm (pump) to the upper arm (probe) in the FUT; while the CSDS provides balanced SBS gain and loss (i.e., no amplification). The successive generation of the CSSS to CSDS is periodically switched by a 10 kHz electronic square wave biasing the DMZM. The amplified or unamplified probe wave passes through a variable optical attenuator (VOA) and a photo-detector (PD), which is demodulated by a lock-in amplifier (LIA) referred at the above 10-kHz square wave.

Four silica optical fiber taper samples we studied here are all drawn from the commercial Fujikura FutureGuide SMF by hydrogen flame [21]. The SBS property in the same untapered SMF has been essentially studied, where 4 acoustic resonance peaks were observed and the 4th-order peak is attributed to the 4th-order acoustic mode mostly existing in the pure-silica cladding [22]. Figure 2 illustrates a schematic diagram of the fiber taper with three microscopic images of the waist, intermediate and untapered zones, respectively. Table 1 summarizes the parameters of the fiber tapers. The waist diameters (d_w) are in the range of 5 μm to 42 μm with different taper lengths (l_0) because of the mass conservation rule [23]. Each taper sample is concatenated with two fiber pigtails. The total length and transmission loss of each concatenated taper sample (including the two fiber pigtails and the tapered section) is estimated to be 1 m and ~1 dB, respectively.

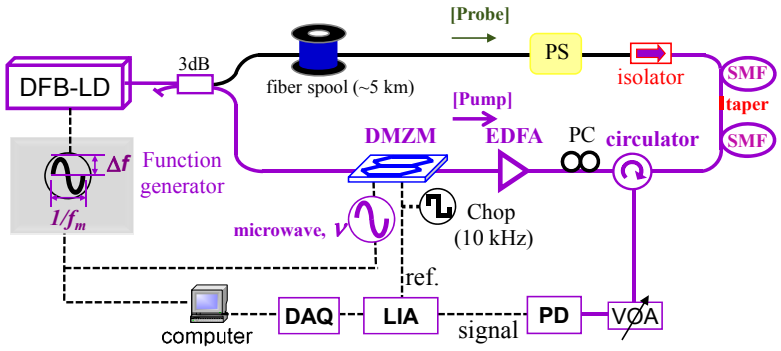

Fig. 1. Experimental setup of characterizing SBS in silica optical fiber tapers. Distributed measurement is implemented by use of a function generator to introduce sinusoidal frequency modulation into the 1550-nm distributed feedback laser diode (DFB-LD). DMZM: dual-parallel Mach–Zehnder modulator; EDFA: erbium-doped fiber amplifier; PC: polarization controller; PS: polarization scrambler; VOA: variable optical attenuator; PD: photo detector; LIA: lock-in amplifier; DAQ: data acquisition card.

#183374 - $15.00 USD Received 14 Jan 2013; revised 8 Feb 2013; accepted 28 Feb 2013; published 7 Mar 2013

Table 1. Parameters of Silica Optical Fiber Tapers

	Sample 1	Sample 2	Sample 3	Sample 4
Taper length l_0 (mm)	28	15	7	5
Waist diameter d_w (μm)	5	13	31	42

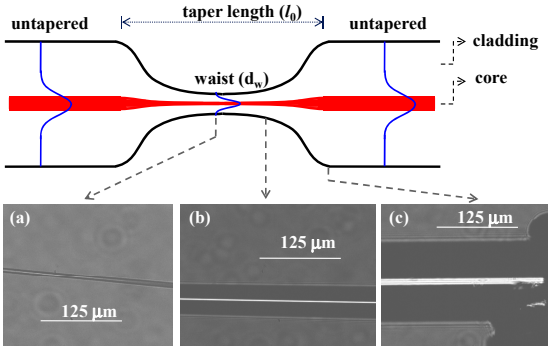

Fig. 2. Schematic diagram of optical fiber taper. (a), (b) and (c) denote the microscopic images of the waist, intermediate and untapered zones, respectively.

3. Results and discussion

We perform two individual experimental studies. First, we study the entire SBS property in the fiber taper with 5 μm waist diameter (Sample 1). Second, we implement the distributed SBS measurement in the Sample 1 as well as the other samples. As will be demonstrated below, the second study is critical to discover the unique characteristics in the fiber tapers, which is attributed to the high spatial resolution of the BOCDA.

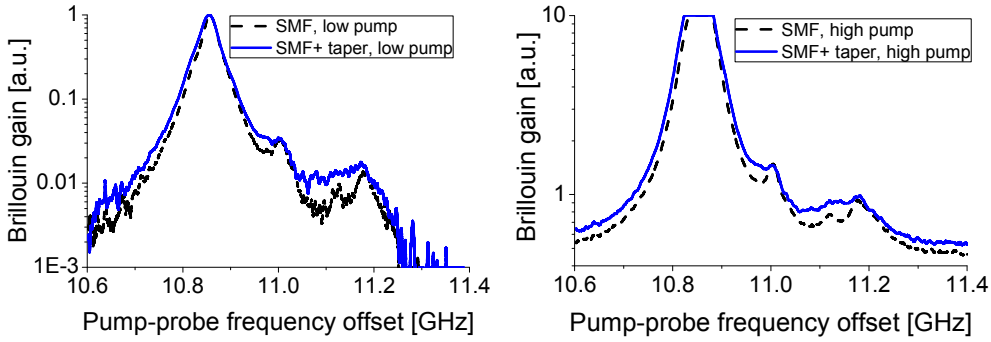

Fig. 3. Measured BGS of FUT with or without fiber taper with 5 μm waist diameter. The total length of each FUT is equal to 1m. (a) pump power = 13 dBm; (b) pump power = 23 dBm.

For the entire SBS property study, the probe power is set at −3 dBm; the pump power is set at 13 or 23 dBm, respectively. For clear comparison, a 1-m-long untapered normal SMF was also measured by the same experimental setup. The measured Brillouin gain spectrum (BGS) is depicted in Fig. 3. It is shown that the BGS of the SMF suffers influence from the fiber taper, typically in the frequency range above ~10.9 GHz. In other words, the Brillouin gain at the higher peaks of the SMF (from ~10.9 GHz to ~11.17 GHz) becomes stronger. Note that the results measured by higher pump power (Fig. 3(a)) is much clearer than those by lower pump power (Fig. 3(b)).

#183374 - $15.00 USD Received 14 Jan 2013; revised 8 Feb 2013; accepted 28 Feb 2013; published 7 Mar 2013

For distributed SBS measurement, a sinusoidal frequency modulation with the modulation depth of Δf = 12 GHz and the modulation frequency around f_m = 20 MHz is introduced into the laser source for distributed SBS measurement based on the BOCDA technique [20]. The spatial resolution and measurement range of the distributed measurement are estimated to be Δz = 4 mm and d_R = 5.2 m, respectively [20]. The scanning step is set to be 0.7 mm by precisely changing the modulation frequency f_m. The optical power of the probe and pump beam is 7 dBm and 23 dBm, respectively.

Figure 4(a) depicts the characterized three-dimensional (3D) BGS distribution in the fiber taper with 5 μm waist diameter. The BFS distribution is evaluated by peak searching of the 3D BGS (see red curve in Fig. 4(b)). It is experimentally demonstrated that the waist of the fiber taper has the greatest BFS of 11.17 GHz, which is exactly the same as the fourth-order resonance frequency of the SMF. The qualitative explanation is described as follows. Since the fiber taper is downscaled from 125 μm to 5 μm, there are a number of optical modes (possibly acoustic modes as well) existing in the taper waveguide although it is called a core-less waveguide structure [1, 23]. This is due to the great contrast of the refractive index and acoustic velocity between the pure silica (i.e., original cladding of the SMF) and surrounding air. It is worth noting that the acoustic modes in fiber tapers will be quite different or more complicated rather than the optical modes because the acoustic velocity of air is far lower than the silica and it could be regarded as an anti-waveguide acoustic structure [24]. Taken into account the fundamental optical mode, the effective refractive index (n_{eff}) is very close to the pure silica for fiber tapers with waist diameter from 5 μm to 50 μm [25, 26]. Similar estimation of the fundamental acoustic mode might provide that its acoustic velocity (V_a) is similar with the pure silica. Therefore, the BFS (i.e., the first acoustic resonance frequency) in the fiber taper's waist is equal to the pure silica. It is the same situation as the fourth-order resonance peak of the SMF [22]. Strict theoretical analysis is required to discover the physical reason.

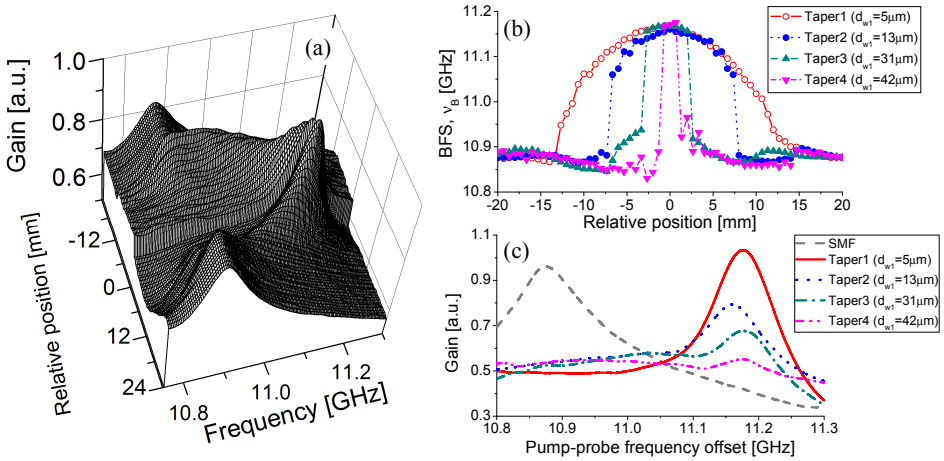

Fig. 4. (a) Example of three dimensional plot of distributed BGS around the fiber taper with ~5 μm waist diameter (Sample 1). (b) Measured BFS distribution around the four fiber tapers; (c) the local BGS in the SMF and the waist of four fiber tapers.

There is a gradual BFS change aside from the taper waist. In the intermediate zone of the fiber taper, the diameter is continuously increased from that of the waist, and the waveguide structure becomes more likely to the Germanium-doped-silica core of the SMF [1, 23]. Consequently, the BFS suffers a gradual change along the fiber taper from 11.17 GHz (the BFS of the taper's waist) to 10.88 GHz (the BFS of the undrawn SMF). This distributed observation can explain the fact that a wide range of the BGS appears in the entire BGS measurement (see Fig. 3). Besides, one can qualitatively see that the Brillouin gain is highest

#183374 - $15.00 USD Received 14 Jan 2013; revised 8 Feb 2013; accepted 28 Feb 2013; published 7 Mar 2013

in the waist but decreases in the intermediate zones. One possible reason is the increase in the geometrical diameter from the waist to the untapered zone [1, 23]. However, more persuasive investigations should be implemented by consideration of the change of optical and acoustic waveguide structure as well as the acousto-optic effective area [11] in the taper sample. Further theoretical and numerical research is needed on this point.

Finally, we studied the BFS distribution in the four taper samples with the waist diameters downscaled from 5 μm to 42 μm. The experimental results are summarized in Fig. 4(b). It shows that all fiber tapers have the greatest BFS of ~11.17 GHz in the waist. However, the BFS distribution in the intermediate zones is sample dependent. For example, the sample with smaller waist has longer-length distribution of the gradually-changed BFS, which matches longer taper length (l_0) (see Table 1). It is interesting that the BFS distribution in the range between the intermediate and untapered zones in Samples 2, 3 and 4 has a dip or an abrupt change. The possible reason is due to the residual stress stored in this range during the stretching process by hydrogen flame although only Sample 4 has a tapering length of l_0 = 5 mm comparable to the spatial resolution (Δz = 4 mm). It is under plan to investigate the effects of annealing to this phenomenon by further improving the spatial resolution Δz (for example, by use of a special LD with much broader modulation depth [27]).

Figure 4(c) compares the local BGS in the waists of all taper samples measured by the BOCDA technique. It can qualitatively indicate that there is quite difference in their Brillouin gain. In other words, smaller waist diameter contributes to greater Brillouin gain. Next study should be performed on exploration of both optical and acoustic waveguide structure in all taper samples so as to know the influence on the acousto-optic effective area as well as the Brillouin gain [11].

4. Conclusion

The SBS property in the silica optical fiber tapers has been experimentally characterized. The tapers were all drawn from the same commercial SMF by hydrogen flame with different waist diameters downscaled from 5 μm to 42 μm. Either entire or distributed SBS measurement was investigated. Thanks to distributed SBS measurement with millimeter spatial resolution based on the BOCDA technique, the SBS property in the fiber tapers has been able to be essentially explored. The entire SBS measurement shows that the BGS in the untapered normal SMF is enhanced in magnitude from ~10.9 GHz to ~11.17 GHz. The distributed measurement indicates that it is attributed to the gradual change of the BFS along the taper samples, that is, the waist in different fiber tapers possessing the approximately unique BFS of ~11.17 GHz but the intermediate zones suffering the gradual decrease of the BFS. It was observed that different Brillouin gain exists not only in different zones of the same taper but also in different tapers' waists. The physical reason may be due to the change of optical and acoustic waveguide structure in the fiber tapers. Its further theoretical analysis is to be pursued. Considering the unique SBS property in fiber tapers and the commercial availability of precise tapering machines, it is expectable to utilize the fiber tapers for extensive applications in Brillouin-based devices and systems, such as Brillouin fiber lasers, Brillouin amplifiers or the Brillouin distributed sensing etc.

Acknowledgments

This work is supported by the National "973" Program of China (No. 2011CB301700), the National Natural Science Foundation of China (Grant No. 61007052, 61107041, 61127016), the International Cooperation Project from the Ministry of Science and Technology of China (Grant No. 2011FDA11780), Shanghai Pujiang Program (Grant No. 12PJ1405600), Shanghai Excellent Academic Leader Program (Grant No. 12XD1406400), and the "SMC Young Star" Scientist Program of Shanghai Jiao Tong University.

#183374 - $15.00 USD Received 14 Jan 2013; revised 8 Feb 2013; accepted 28 Feb 2013; published 7 Mar 2013